0026-895X/99/020269-10$3.00/0

MOLECULAR PHARMACOLOGY, **55:**269–278 (1999).

The Steroid Promegestone Is a Noncompetitive Antagonist of the *Torpedo* Nicotinic Acetylcholine Receptor that Interacts with the Lipid-Protein Interface

MICHAEL P. BLANTON,[1] YU XIE,[2] LAWRENCE J. DANGOTT,[3] and JONATHAN. B. COHEN

Department of Neurobiology, Harvard Medical School, Boston, Massachusetts

Received August 24, 1998; accepted October 30, 1998

This paper is available online at http://www.molpharm.org

ABSTRACT

17,21-Dimethyl-19-nor-pregn-4,9-diene-3,20-dione (promegestone) was used to characterize the mechanism of inhibition of nicotinic acetylcholine (ACh) receptors (AChR) by progestin steroids. Promegestone reversibly inhibited ACh-induced currents of *Torpedo* AChRs expressed in *Xenopus* oocytes. Between 1–30 μM promegestone produced a concentration-dependent enhancement of the equilibrium binding affinity of [^{3}H]ACh to *Torpedo* AChR-rich membranes. For AChRs in the presence of agonist (desensitized state) promegestone was a more potent inhibitor of the binding of the noncompetitive antagonist [^{3}H]phencyclidine (IC_{50} = 9 μM) than of [^{3}H]histrionicotoxin (IC_{50} ~ 100 μM). To identify AChR domains in contact with the steroid, AChR-rich membranes equilibrated with [^{3}H]promegestone were irradiated at 312 nm, and ^{3}H-labeled amino acids were identified by amino-terminal sequencing of fragments isolated from subunit proteolytic digests. Within AChR α-subunit, 70% of ^{3}H was covalently incorporated in a 10-kDa fragment beginning at Asn-339 and containing the M4 membrane spanning segment, and 30% was in a 20-kDa fragment beginning at Ser-173 and containing the M1–M3 segments. Fragments containing the M2 channel domains as well as the M4 segments were isolated from proteolytic digests of AChR subunits and subjected to amino-terminal sequence analysis. No evidence of [^{3}H]promegestone incorporation was detected in any of the M2 segments. The amino acids in the M4 segments labeled by [^{3}H]promegestone were among those previously shown to be in contact with the lipid bilayer (Blanton and Cohen, 1994). These results indicate that the steroid promegestone is an AChR noncompetitive antagonist that may alter AChR function by interactions at the lipid-protein interface.

Steroid hormones, including endogenously occurring metabolites of progesterone, testosterone, and deoxycorticosterone, as well as synthetic derivatives, act as allosteric modulators of the nicotinic acetylcholine (ACh) receptor (AChR) family of ligand-gated ion channels (reviewed in Franks and Lieb, 1994; MacDonald and Olsen, 1994; Lambert et al., 1995). Progesterone is a weak allosteric potentiator of type A γ-aminobutyric acid ($GABA_A$) receptors (Wu et al., 1990), whereas endogenous and synthetic 3α-hydroxy derivatives act at submicromolar concentrations (Harrison et al., 1987; Gee et al., 1995). In contrast, at micromolar concentrations progesterone and its derivatives inhibit ACh-activated responses of both neuronal and muscle-type AChRs (Gillo and Lass, 1984; Valera et al., 1992; Ke and Lukas, 1996; Bullock et al., 1997) as well as glycine receptor-activated currents in spinal cord neurons (Wu et al., 1990). For $GABA_A$ receptors electrophysiological studies show that potentiation by steroids is not associated with changes in channel conductance but with an increase in open channel probability at low agonist concentrations and an alteration of the kinetics of desensitization at high agonist concentrations (Twyman and MacDonald, 1992; Lambert et al., 1996; Zhu and Vicini, 1997). For muscle AChR, single-channel analyses of the acute effects of hydrocortisone and corticosterone indicate a dose-dependent decrease in the mean channel open time

This research was supported in part by U.S. Public Health Service Grant GM 15904 and by an award in Structural Neurobiology from the Keck Foundation.

[1] Current address: Department of Pharmacology, Texas Tech University of Health Sciences Center, Lubbock, TX 79430.

[2] Current address: Millenium Pharmaceuticals, Cambridge, MA 02139.

[3] Current address: Protein Chemistry Laboratory, Department of Chemistry, Texas A&M University, College Station TX 77842.

ABBREVIATIONS: ACh, acetylcholine; AChR, nicotinic acetylcholine receptor; Promegestone, 17,21-dimethyl-19-nor-pregn-4,9-diene-3,20-dione; 1-AP, 1-azidopyrene; PAGE, polyacrylamide gel electrophoresis; HPLC, high-performance liquid chromatography; NCA, noncompetitive antagonist; HTX, *d,l*-perhydrohistrionicotoxin; [^{125}I]TID, 3-(trifluoromethyl)-3(*m*-[^{125}I]iodophenyl)diazirine; EKC, endoproteinase Lys-C; PCP, phencyclidine; PTH, phenylthiohydantoin; TPS, *Torpedo* physiological saline (250 mM NaCl, 3 mM $CaCl_2$, 2 mM $MgCl_2$, 5 mM sodium phosphate, pH 7.0); T, total acrylamide concentration; C, bis-acrylamide cross-linker concentration relative to total acrylamide concentration; GABA AChR, γ-aminobutyric acid; αV8–20, 20-kDa V8 protease fragment of the AChR α-subunit; αV8–10, 10-kDa V8 protease fragment of the α-subunit.

(Bouzat and Barrantes, 1996; Nurowska and Ruzzier, 1996). Although a mutation within the M2 ion channel domain that increases channel lifetime also increases hydrocortisone potency, there was no evidence for hydrocortisone competition with QX-222, an open channel blocker (Bouzat and Barrantes, 1996). Because substitutions of amino acids within AChR M4 hydrophobic segments at the lipid-protein interface can result in alteration of the duration of the open channel state (Bouzat et al., 1994; Lee et al., 1994; Lasalde et al., 1996), it is possible that steroid interactions with the AChR at the lipid interface result in functional antagonism.

To identify binding sites for progestin steroids in AChRs, we have characterized interactions of 17,21-dimethyl-19-norpregn-4,9-diene-3,20-dione (promegestone) with AChR-rich membranes isolated from the electric organ of the marine elasmobranch *Torpedo californica*. UV irradiation of promegestone results in the formation of a triplet-state biradical at the 3′ ketone allowing a covalent bond to be formed between the steroid and an adjacent polypeptide (Benisek, 1977). Photoincorporation of [^{3}H]promegestone has been used to identify several different progesterone receptors (Sadler and Maller, 1982; Stromstedt et al., 1990). The *Torpedo* electric organ is an extremely rich source of muscle-type AChR containing upwards of 100 mg of receptor protein/kg electroplacque tissue, thus facilitating the use of protein chemistry techniques to identify sites of photoincorporation of competitive and noncompetitive antagonists (reviewed in Hucho et al., 1996).

We report here that promegestone reversibly inhibits ACh-evoked currents of *Torpedo* AChR expressed in *Xenopus* oocytes and that it interacts with both the resting and desensitized states of the AChR, inhibiting the specific binding of radiolabeled noncompetitive antagonists to *Torpedo* AChR-rich membranes in the absence and in the presence of carbamylcholine, respectively. [^{3}H]Promegestone photoincorporates into each of the AChR subunits with the extent of incorporation insensitive to AChR conformational state. No evidence of [^{3}H]promegestone incorporation was detected in any of the channel lining M2 segments, but labeled residues were identified in the M4 hydrophobic segments at positions shown previously to be at the AChR-lipid interface. These results support the hypothesis that inhibition of AChRs by progestin steroids results from direct interactions at the AChR-lipid interface.

Materials and Methods

Materials. [^{3}H]Promegestone (86.7 Ci/mmol; Fig. 1), nonradioactive promegestone, and [^{3}H]phencyclidine ([^{3}H]PCP; 52 Ci/mmol) were obtained from New England Nuclear (Boston, MA). [^{3}H]Tetracaine (36 Ci/mmol) and [^{3}H]histrionicotoxin ([^{3}H]HTX, 60 Ci/mmol) were prepared at New England Nuclear by the tritium gas catalytic reduction of 3,5 dibromotetracaine and *dl*-decahydro(pentyl)histrionicotoxin, respectively. [^{3}H]HTX was diluted with *dl*-perhydrohistrionicotoxin (HTX) to a radiochemical specific activity of 3 Ci/mmol for binding assays. 1-Azidopyrene (1-AP) was purchased from Molecular Probes (Eugene, OR). L-1-tosylamido-2-phenylethyl chloromethyl ketone-treated trypsin was purchased from Worthington Biochemical Corp. (Freehold, NJ), endoproteinase Lys-C (EKC) from Boehringer Mannheim (Indianapolis, IN) and Genapol C-100 (10%) from Calbiochem (La Jolla, CA). Prestained low molecular weight gel standards were purchased from Life Technologies, Inc. (Gaithersburg, MD)

AChR-Rich Membranes. AChR-rich membranes were isolated from the electric organ of *T. californica* (Marinus, Inc., Westchester, CA) as described previously (Pedersen et al., 1986). The final membrane suspensions in 36% sucrose/0.02% NaN_3 were stored at −80°C under argon and contained 1–1.5 nmol of ACh binding sites/mg of protein as measured by a direct [^{3}H]AChR binding assay (Pedersen et al., 1986).

Electrophysiological Recordings. Plasmid cDNAs (pMXT) encoding wild-type α-,γ-, and δ-subunits of *Torpedo* AChR were gifts from Dr. Michael White (Allegheny Health Sciences University, Philadelphia, PA), and the β-subunit cDNA (pSP64 vector) was from Dr. Henry Lester (California Institute of Technology, Pasadena, CA). cDNAs were linearized with either *Xba*I (for α-, γ-, and δ-subunits) or *Fsp*I (for β-subunit). Linear DNAs were transcribed in vitro with SP6 RNA polymerase (Promega, Madison, WI). Isolated follicle-free oocytes were microinjected with 10 ng of subunit-specific RNAs in a molar ratio of $\alpha_2\beta\gamma\delta$. Oocytes were maintained in low-Ca^{++} ND96 solution containing 96 mM NaCl, 2 mM KCl, 0.3 mM $CaCl_2$, 1 mM $MgCl_2$, 5 mM HEPES ,and 50 μg/ml gentamicin (pH 7.6) for at least 48 h before use. Currents elicited by ACh were measured with a standard two-electrode voltage-clamp (OC-725B, Warner Instrument Corp., Hamden, CT) at a holding potential of −70 mV. Electrodes were filled with 3 M KCl and had resistance of 0.5–3.0 MΩ. The recording chamber (~150 μl in volume) was continually perfused by gravity with low-Ca^{++} ND96 (+1 μM atropine, pH 7.6). Stock solutions of steroid were prepared in ethanol and then diluted in low-Ca^{++} ND96 so that the oocytes were exposed to ethanol concentrations <1% (v/v). Various concentrations of steroid were applied simultaneously with 3 μM ACh for 5 s through solenoid valves to the oocyte in the recording chamber. In some experiments, progesterone was perfused continuously through the chamber for up to 5 min, with responses to ACh tested periodically.

Binding of Cholinergic Ligands to AChR-Rich Membranes. Centrifugation assays were used to determine the equilibrium binding of [^{3}H]ACh, [^{3}H]HTX, [^{3}H]PCP, and [^{3}H]tetracaine to *Torpedo* AChR-rich membranes in *Torpedo* physiological saline (TPS; 250 mM NaCl, 5 mM KCl, 3 mM $CaCl_2$, 2 mM $MgCl_2$, 5 mM sodium phosphate, pH 7.0.). The final concentration of ethanol was <0.3% (v/v) for [^{3}H]ACh or equal to 1% (v/v) for the ^{3}H noncompetitive antagonists. For [^{3}H]ACh, membrane suspensions (50 μg/ml of protein, 50 nM ACh binding sites) were pretreated with 0.3 mM diisopropylphosphofluoridate to inhibit acetylcholinesterase. Membranes were equilibrated at 4°C with [^{3}H]ACh (50 nM) and varying concentrations of noncompetitive antagonist for 30 min, and 0.5 ml aliquots were centrifuged for 45 min at 10,000 rpm in a Sorvall SA-600 rotor. After complete removal of the supernatant, membrane pellets were resuspended in 0.1 ml of 10% SDS and pellet ^{3}H was determined by liquid scintillation counting. For the ^{3}H noncompetitive antagonists, membrane suspensions (0.5 mg of protein/ml, 0.6 μM ACh binding

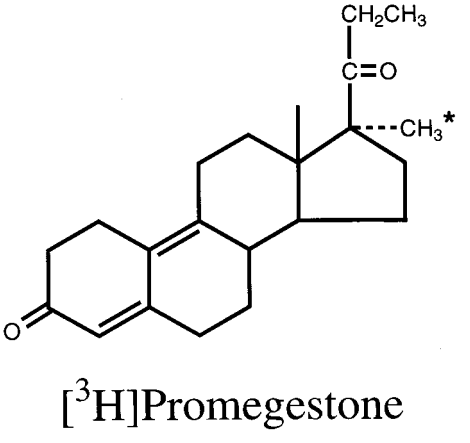

Fig. 1. Structure of [^{3}H]promegestone [17α-methyl-^{3}H]

sites) were equilibrated with radioligand and appropriate concentrations of modulatory drug for 2–3 h at room temperature ([^{3}H]HTX, 10 nM) or at 4°C ([^{3}H]PCP, 6 nM; [^{3}H]tetracaine, 2 nM) before centrifugation. Nonspecific binding of [^{3}H]ACh was measured in the presence of 0.1 mM carbamylcholine, that of [^{3}H]HTX and [^{3}H]PCP in the presence of 0.2 mM meproadifen, and that of [^{3}H]tetracaine in the presence of 0.2 mM tetracaine.

Photolabeling AChR-Rich Membranes with [^{3}H]Promegestone. Membranes in TPS (2 mg of protein/ml) were incubated with [^{3}H]promegestone at a final concentration 80–110 nM in the absence or presence of 0.2 mM carbamylcholine. After a 1-h incubation, suspensions were irradiated for 7 min at a distance of <1 cm with a 312-nm lamp (EB-Spectroline, Spectronics, Westbury, NY). Each sample was then pelleted (15,000*g*), and for analytical labelings the pellets were then solubilized in sample loading buffer (Laemmli, 1970) and submitted to SDS-polyacrylamide gel electrophoresis (PAGE). For preparative scale labelings (12–15 mg of AChR-rich membranes), the pellets were then resuspended in TPS at 2 mg/ml of protein and 1-AP was added to a final concentration of 350 μM. After a 30-min incubation, membranes were once again irradiated (365 nm for 5 min, at <1 cm; EN-Spectroline,) and each sample was pelleted. Samples were then solubilized in electrophoresis sample loading buffer and submitted to preparative scale SDS-PAGE. Labeling with the fluorescent hydrophobic probe 1-AP was used to assist in the initial identification and isolation of AChR subunits and in the subsequent isolation of hydrophobic segments of these subunits (Blanton and Cohen, 1994).

SDS-PAGE. SDS-PAGE was performed as described (Laemmli, 1970) with either 1.0-mm (analytical) or 1.5-mm thick (preparative scale) 8% T (total acrylamide concentration), 4% bis-acrylamide cross-linker concentration relative to total acrylamide concentration (C). For analytical gels, polypeptides were visualized by staining with Coomassie blue *R*-250 (0.25% w/v in 45% methanol and 10% acetic acid) and destaining in 25% methanol and 10% acetic acid. The gels were then impregnated with fluor (Amplify; Amersham, Arlington Heights, IL) for 20 min with rapid shaking, dried, and exposed at −80°C to X-OMAT LS film (Eastman Kodak Co., Rochester, NY) for various times (4–16 weeks). For preparative scale gels, polypeptides incorporating 1-AP were visualized from their associated fluorescence when the gels were illuminated at 365 nm on a UV-light box. Bands corresponding to AChR subunits were excised either for polypeptide isolation or in the case of the AChR α-subunit for proteolytic digestion once the gel piece was transferred to the well of a 15% mapping gel (Cleveland et al., 1977; Pedersen et al., 1986). Mapping gels were composed of a 4.5% T, 2.6% C stacking gel and a 15% T, 2.6% C separating gel. The α-subunit gel piece was overlaid with 350 μl of buffer (5% sucrose, 125 mM Tris-HCl, 0.1% SDS, pH 6.8) containing 250 μg of *Staphylococcus aureus* V8 protease. Electrophoresis was carried out overnight at 15 mA constant current.

1-AP/[^{3}H]promegestone-labeled proteolytic fragments were isolated from the excised gel pieces by a passive elution protocol as described in (Blanton and Cohen, 1994). The eluate was filtered (Whatman 1), and the protein concentrated with a Centriprep-10 (Amicon, Inc., Beverly, MA). Excess SDS was removed by acetone precipitation (overnight at −20°C).

Purification of Proteolytic Digests of [^{3}H]Promegestone/1-AP-Labeled AChR Subunits. For EKC digestion, the acetone-precipitated 20-kDa V8 protease fragment of the α-subunit (αV8–20; Ser-173–Glu-338) was resuspended in 15 mM Tris-HCl, 0.1% SDS (pH 8.1), at 1–2 mg/ml protein. Approximately 1.5 U of EKC were added and incubated at room temperature for 6 days. The β- and δ-subunits and the 10-kDa fragment of the α-subunit (αV8–10) (Asn-339–Gly-437) were digested with trypsin exactly as described (Blanton et al., 1998). Both trypsin and EKC digests were separated on individual 1.5-mm thick 16.5% T, 6% C tricine SDS-PAGE gels (Schagger and von Jagow, 1987; Blanton et al., 1998).

Proteolytic fragments containing either the M2 or M4 region of each of the receptor subunits were identified and isolated by two different sets of criteria: Under conditions nearly identical with those used here, it has been previously determined where proteolytic fragments containing the M2 and M4 regions migrate relative to Life Technologies (GIBCO/BRL, Gaithersburg, MD) prestained molecular weight standards (White and Cohen, 1992; Pedersen et al., 1992; Blanton et al., 1998). In addition, fragments were selected that contain both the M2 and M3 region so that incorporation of 1-AP into the M3 segment (Blanton and Cohen, 1994) could be used to visualize the fragments by illuminating the tricine SDS-PAGE gel at 365 nm on a UV-light box. Incorporation of 1-AP into the M4 segment was also used as an aid in identifying fragments containing this region.

1-AP/[^{3}H]promegestone-labeled fragments were further purified by reverse-phase high-pressure liquid chromatography (HPLC) as described (Blanton et al., 1998) with a Brownlee Aquapore C_4 column (100 × 2.1 mm). Solvent A was 0.08% trifluoroacetic acid in water, and solvent B was 0.05% trifluoroacetic acid in 60% acetonitrile/40% 2-propanol. The elution of [^{3}H]promegestone was monitored by scintillation counting of an aliquot (25 μl) of each 0.5-ml fraction.

Sequence Analysis. Amino-terminal sequence analysis was performed on a ABI model 477A (Applied Biosystems, Foster City, CA) protein sequencer with gas phase cycles. Pooled HPLC samples were dried by vacuum centrifugation, resuspended in a small volume of 0.05% SDS (~20 μl), and immobilized on chemically modified glass fiber disks (Beckman Instruments). Approximately 30% of the released phenylthiohydantoin (PTH)-amino acids were separated by an on-line model 120A PTH-amino acid analyzer, and ~60% was collected for determination of released ^{3}H by scintillation counting of each sample for three 5-min intervals. Initial yield (I_o) and repetitive yield (R) were calculated by nonlinear least-squares regression of the observed release (M) for each cycle (n): $M = I_o R^n$ (PTH-derivatives of Ser, Thr, Cys, and His were omitted from the fit).

Results

To determine whether promegestone was an antagonist of *Torpedo* AChRs, we tested it as an inhibitor of AChRs expressed in *Xenopus* oocytes. When coapplied for 5 s with ACh, promegestone produced a dose-dependent and reversible inhibition of the ACh-induced currents (Fig. 2A). In the absence of promegestone, the ACh concentration-response relation was characterized by K_{ap} = 20 μM and a Hill coefficient of 1.8 (data not shown). When applied in the presence of 3 μM ACh, 30 μM promegestone produced ~50% reduction of the peak current response, whereas that same concentration resulted in a 90% reduction of the current seen after 5 s exposure. After a 1-min wash after exposure to 30 μM promegestone, there was a 50% recovery of the ACh peak current and a full recovery within 5 min. The potency of promegestone as well as its kinetics of inhibition were similar to that of progesterone (Fig. 2B). Although the time-dependent decrease of the ACh-response could indicate that both steroids increase the rate of agonist-dependent desensitization, it was also possible that neither steroid equilibrated with its binding site during the 5 s exposure. To determine whether kinetic factors were important determinants of the extent of inhibition seen for these drugs, ACh responses were determined after preincubation with progesterone. When oocytes were perfused with 1 μM progesterone for 5 min, there was a dramatic, time-dependent increase in progesterone potency, with 50% inhibition of the peak current seen after a 60-s preincubation (Fig. 2C). After 5 min, the peak current was reduced by 65%, and after a 2.5-min wash, there was a 40% recovery of the peak response (not shown). Although further experimentation is required to analyze the time and concentration dependence of the observed

inhibition, these first experiments established that promegestone was in fact an AChR antagonist similar in potency and action to progesterone.

Effects of Promegestone on [^{3}H]ACh and ^{3}H-Noncompetitive Antagonist Binding to Torpedo Membranes. Equilibrium binding of [^{3}H]ACh was assayed at a concentration sufficient to occupy ~20% of sites. At this subsaturating concentration, the assay is sensitive to drugs that either increase or decrease ACh binding affinity (Boyd and Cohen, 1984). Promegestone at concentrations up to 100 μM did not inhibit the equilibrium binding of [^{3}H]ACh, and, in fact, at concentrations between 1 and 30 μM it increased binding by 50% (Fig. 3A). In comparison, proadifen, an aromatic amine noncompetitive antagonist known to stabilize the desensitized state of the AChR (Boyd and Cohen, 1984), increased [^{3}H]ACh binding by 300%.

Promegestone was also tested as an inhibitor of the equilibrium binding of radiolabeled, positively charged AChR noncompetitive antagonists (NCAs) (Fig. 3B). [^{3}H]HTX is bound at equilibrium with high affinity to a single site in the AChR in the absence (resting state, K_{eq} = 1 μM) or presence of agonist (desensitized state, K_{eq} = 0.3 μM) (Heidmann et al., 1983). [^{3}H]Phencyclidine ([^{3}H]PCP) binds with high affinity (K_{eq} = 1 μM) to a single site per AChR in the desensitized state (Heidmann et al., 1983). [^{3}H]Tetracaine binds with high affinity (K_{eq} = 0.3 μM) in the absence of agonist to

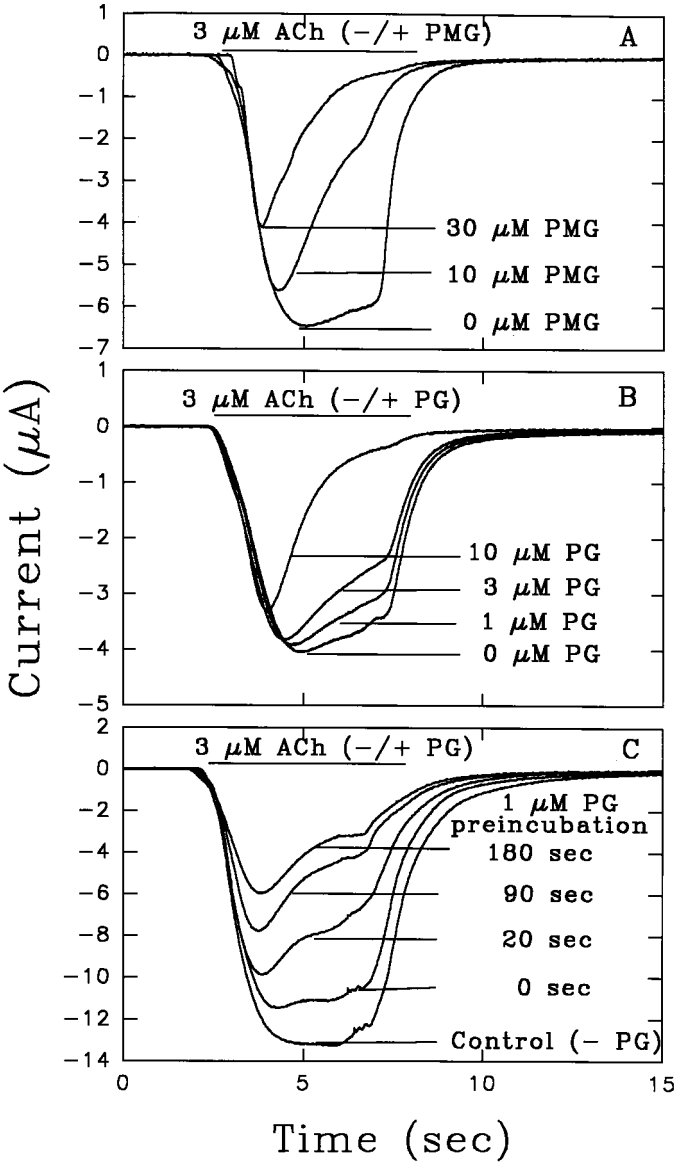

Fig. 2. Inhibition of ACh-evoked currents of *Torpedo* AChRs expressed in *Xenopus* oocytes by promegestone and progesterone. Currents elicited by ACh from *Torpedo* AChRs expressed in *Xenopus* oocytes were measured with a standard two-electrode voltage clamp at a holding potential of −70 mV. A, once a stable response was observed for 3 μM ACh, responses were measured when ACh was applied simultaneously for 5 s with 10 and then 30 μM promegestone, or B, with 1, 3, and then 10 μM progesterone. Inhibition by promegestone and progesterone was reversible, because peak responses to ACh returned to control levels after exposure to 30 μM promegestone or to 10 μM progesterone (not shown). C, current response was recorded when 3 μM ACh was applied for 5 sec (Control), and then progesterone (1 μM) was applied continuously for 5 min, with test pulses of 3 μM ACh (and progesterone) at the indicated times. After 5 min exposure, the peak current was reduced to 35% of control, and after a 2.5 min wash there was a recovery to 60% of control (not shown).

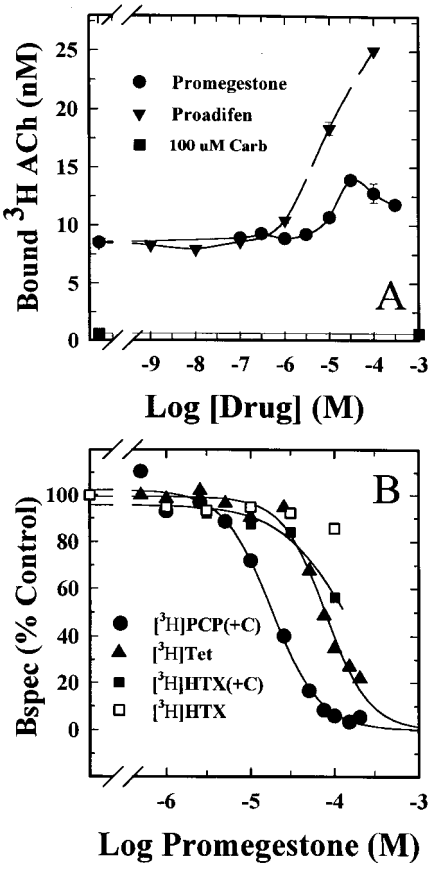

Fig. 3. Effects of promegestone on the equilibrium binding of [^{3}H]ACh, [^{3}H]histrionicotoxin, [^{3}H]phencyclidine, and [^{3}H]tetracaine. A, AChR-rich membranes suspensions (50 μg protein/ml, 50 nM ACh binding sites), pretreated with diisopropylphosphofluoridate, were equilibrated at 4°C for 30 min with [^{3}H]ACh (50 nM) and promegestone (●) or proadifen (▲), and bound [^{3}H]ACh was determined by a centrifugation assay. B, AChR membranes (0.5 mg/ml, 0.6 μM ACh binding sites) were equilibrated at room temperature for 2 to 3 h with 10 nM [^{3}H]HTX in the absence (□) or presence (■) of carbamylcholine, with 6 nM [^{3}H]PCP in the presence of carbamylcholine (●), or with 2 nM [^{3}H]tetracaine (▲) and the indicated concentrations of promegestone. Specific binding was determined as the difference between the total binding and the nonspecific binding in the presence of either 200 μM tetracaine (for [^{3}H]tetracaine) or 200 μM meproadifen. In the absence of promegestone, [^{3}H]HTX total binding was 4000 ^{3}H cpm in the absence and 4200 in the presence of carbamylcholine, and 350 ^{3}H cpm were bound nonspecifically. For [^{3}H]PCP, total and nonspecific binding were 15,000 and 2,500 ^{3}H cpm, respectively, and for [^{3}H]tetracaine they were 69,200 and 22,500 cpm.

a single site per AChR and it is bound only weakly (K_{eq} = 30 μM) in the desensitized state (Cohen et al., 1985). Based on photoaffinity labeling, the [^{3}H]tetracaine binding site has been localized within M2 ion channel domain (Gallagher and Cohen, 1994; Gallagher, 1996). In the presence of agonist, promegestone was a potent inhibitor of [^{3}H]PCP binding. High concentrations inhibited specific binding by >95%, and the concentration dependence of inhibition could be modeled as competitive with IC_{50} = 9 μM (Fig. 3B). In contrast, 100 μM promegestone did not inhibit [^{3}H]HTX binding in the absence of agonist and produced only partial inhibition in the presence of agonist. For [^{3}H]tetracaine in the absence of agonist, high concentrations of promegestone inhibited binding by at least 80% with an IC_{50} of 75 μM.

Photoincorporation of [^{3}H]Promegestone in the AChR. Experiments were first designed to characterize the general pattern of [^{3}H]promegestone photoincorporation into *Torpedo* AChR-rich membranes, as well as to test the sensitivity of the photoincorporation to cholinergic ligands. Membranes (2 mg/ml) were equilibrated with 80 nM [^{3}H]promegestone in the absence and in the presence of 200 μM carbamylcholine. This promegestone concentration provided a sufficient level of radioactivity to detect AChR subunit labeling even though only a small amount of the total ^{3}H (~2%) was incorporated. After irradiation, membrane suspensions were pelleted and resuspended in electrophoresis sample buffer, and the pattern of incorporation was monitored by SDS-PAGE followed by fluorography. As is evident in the fluorograph of an 8% polyacrylamide gel (Fig. 4), there was incorporation of [^{3}H]promegestone into each of the AChR subunits. Neither the pattern of incorporation into individual AChR subunits nor the overall labeling pattern was affected by the inclusion of 200 μM carbamylcholine (Fig. 4, lane 2). The additional presence of nonradioactive progesterone (1.2 μM, 12 μM, and 100 μM) had no observable effect on the extent of incorporation into any of the AChR subunits either in the presence or absence of agonist (data not shown). Based upon quantification of ^{3}H incorporation in excised gel slices, ~0.1% of α-subunits were labeled with the relative incorporation within subunits: $\alpha/\beta/\gamma/\delta$:1.6/1.1/1.2/1 in the absence of agonist. Similar ratios were seen for photolabeling in the presence of agonist as well as from the amount of ^{3}H present in subunits isolated from preparative scale labelings.

The distribution of [^{3}H]promegestone incorporation within the AChR α-subunit was examined by determining the amount of labeling in two large proteolytic fragments generated by limited *S. aureus* V8 protease digestion on a mapping gel: αV8–20 (Ser-173–Glu-338), containing the membrane spanning segments M1–M3, and αV8–10 (Asn-339–Gly-439), containing the membrane spanning segment M4 (Pedersen et al., 1986; White and Cohen, 1988). In the fluorograph of an analytical mapping gel all the visible labeling was contained within αV8–10. However, scintillation counting of the material contained within these two α-subunit fragments, isolated from preparative scale labelings, indicated that ~70% of ^{3}H cpm was incorporated in αV8–10 and 30% was in αV8–20. The relative incorporation of [^{3}H]promegestone into αV8–10 was similar for labelings carried out in the absence (74%) and in the presence (70%) of 200 μM carbamylcholine.

Identification of the Sites of [^{3}H]Promegestone Incorporation in the M4 Segments of the α, β, and γ AChR Subunits. The M4 segments from AChRs labeled with [^{3}H]promegestone in the presence of 200 μM carbamylcholine were isolated from tryptic digests of either the intact subunit (β, γ, ~250 μg) or αV8–10 (~125 μg). When the tryptic digest of α-V8–10 was purified by reverse-phase HPLC, ^{3}H counts eluted in a peak centered at ~82% solvent B (Fig. 5A) along with the peak of 1-AP fluorescence (data not shown). Amino-terminal sequence analysis (Fig. 6A) of the pool of HPLC fractions 31–35 revealed the presence of a primary sequence beginning at αTyr-401 (initial yield, 129 pmol) present at 15-fold higher level than a secondary sequence that began at αSer-388. In the pattern of ^{3}H release shown in Fig. 6A, there were 620 cpm released in the first cycle, equivalent to 1.5% of loaded cpm and similar in magnitude to the 1.3% of ^{3}H cpm washed off the filter by acid treatment before the first cycle of Edman degradation (data not shown). The progressively declining ^{3}H release seen in the first 4 cycles of Edman degradation was likely to result either from release of peptide poorly adsorbed on the glass

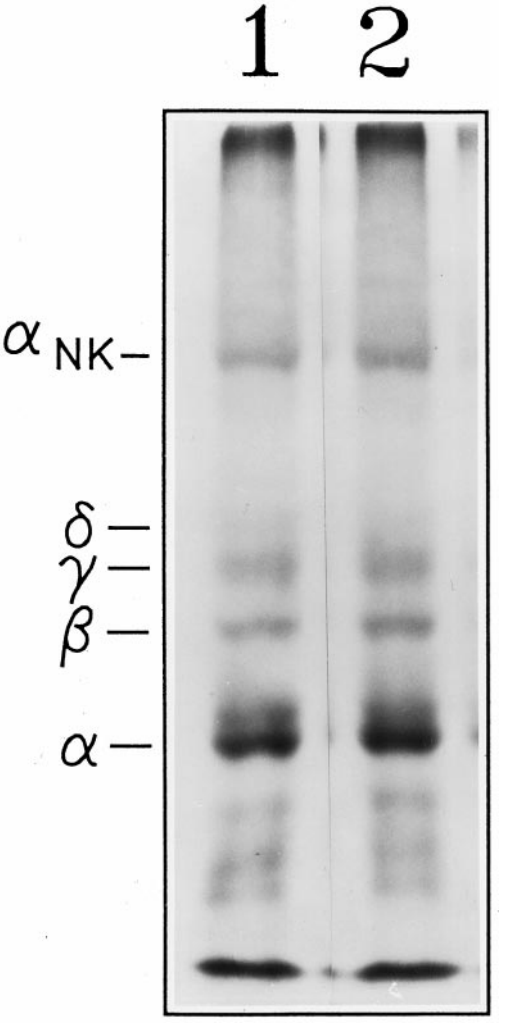

Fig. 4. Photoincorporation of [^{3}H]promegestone into AChR-rich membranes in the absence and in the presence of carbamylcholine. AChR-rich membranes were equilibrated with 80 nM [^{3}H]promegestone in the absence (lane 1) or presence (lane 2) of 200 μM carbamylcholine and irradiated at 312 nm for 7 min. After photolysis, polypeptides were resolved on a 8% polyacrylamide gel and processed for fluorography (5-week exposure). The bulk of the labeled lipid and free photolysis products were electrophoresed from the gel with the tracking dye. AChR subunits and the Na^+/K^+ ATPase α-subunit (α_{NK}) are indicated on the left.

support or chemical instability of some incorporated ^{3}H. A stable baseline of ^{3}H release was achieved by cycle 5, and, in addition to the prominent ^{3}H release in cycle 12, there was also clear, but lower level, release in cycles 8 and 18. Comparison of the pattern of release with the corresponding amino acids in the primary sequence indicates that the labeled amino acids include His-408 (0.7 cpm/pmol), Cys-412 (9 cpm/pmol), and Cys-418 (2 cpm/pmol). These same three residues were found to have incorporated [^{3}H]promegestone when the M4 region was isolated from membranes labeled in the absence of agonist (data not shown). Cys-412 is the residue in αM4 at the lipid interface that is labeled most efficiently by the hydrophobic probes 3-(trifluoromethyl)-3(*m*-[^{125}I]iodophenyl)diazirine[^{125}I](TID) and [^{3}H]diazofluorene; Cys-418 is labeled by both probes, and His-408 is labeled only by [^{3}H]diazofluorene (Blanton and Cohen, 1994; Blanton et al., 1998).

Tryptic digestion of the intact β-subunit produced on a tricine SDS-PAGE gel a fluorescent and radioactive band migrating with an apparent molecular mass of 4 kDa (βT-4K), known to contain the βM4 region (Blanton et al., 1998), which was further purified by HPLC (Fig. 5C). Amino-terminal sequence analysis (Fig. 6B) of the pooled fractions (28–32) revealed the presence of a primary sequence beginning at βAsp-427 (129 pmol) as well as a secondary sequence beginning at the amino terminus of βM1 (βLys-216, 40 pmol). As with αM4, recovery of ^{3}H in the acid prewash and in cycle 1 were each equal to 1% of ^{3}H cpm loaded. A stable baseline of ^{3}H release was seen in cycles 5–14, followed by prominent ^{3}H release in cycle 15 with additional release in cycle 21. A comparison of the pattern of ^{3}H release with the corresponding amino acids identified in the peptide beginning at βAsp-427 indicate that Tyr-441 (0.5 cpm/pmol) and Cys-447 (0.2 cpm/pmol) are labeled, the same residues in βM4 that were labeled nonspecifically by [^{125}I]TID (Blanton and Cohen, 1994) and by [^{3}H]diazofluorene (Blanton et al., 1998).

When the tryptic digest of the intact [^{3}H]promegestone-labeled γ-subunit was resolved on a tricine SDS-PAGE gel, a band of fluorescence and ^{3}H migrated with an apparent molecular mass of 5 kDa (γT-5K). Material eluted from the γT-5K band was further purified by reverse-phase HPLC (Fig. 5E) with peaks of both 1-AP fluorescence and ^{3}H counts eluting at 75% solvent B. Amino-terminal sequence analysis of the pool of fractions 28–32 revealed the presence of a primary sequence (Fig. 6C) beginning at γVal-446 and ex-

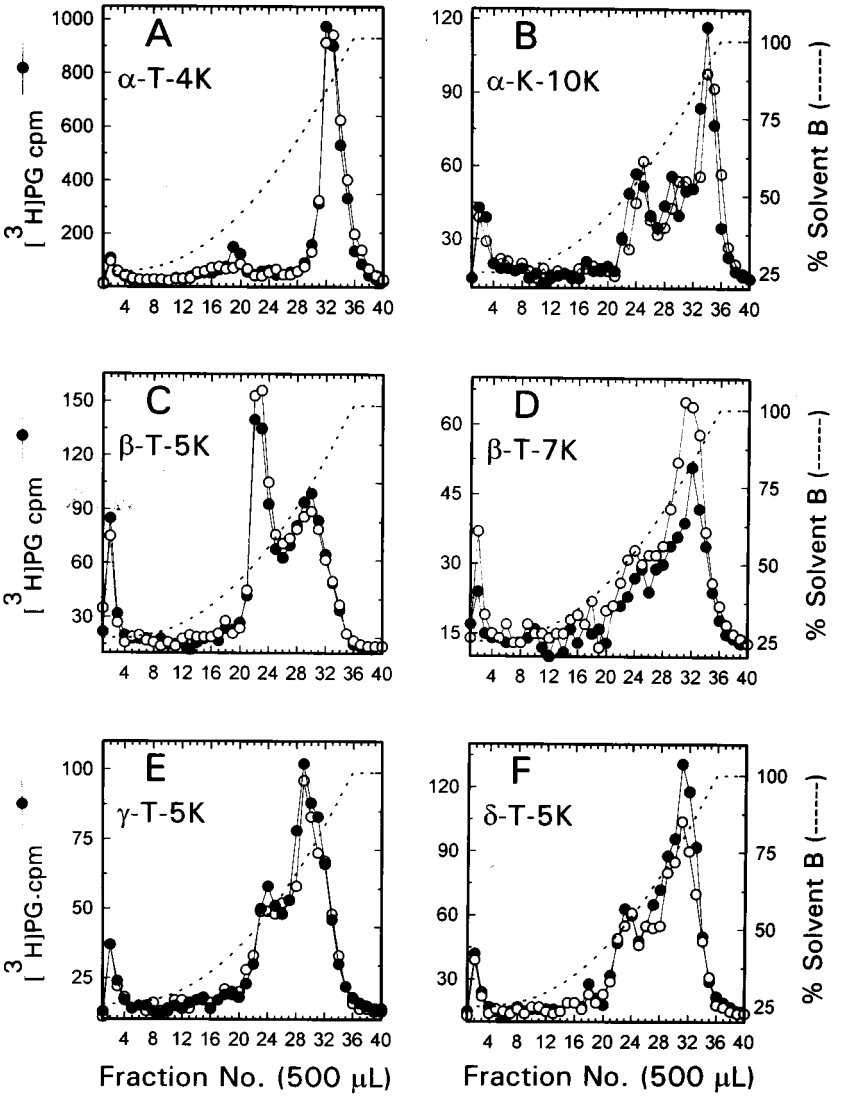

Fig. 5. Reverse-phase HPLC purification of proteolytic fragments of [^{3}H]promegestone-labeled AChR subunits containing M4 and M2 hydrophobic segments. AChR subunits were isolated from AChR-rich membranes (12 mg protein) labeled with [^{3}H]promegestone in the presence of carbamylcholine and in the absence (●) or presence (○) of 60 μM phencyclidine. Proteolytic digests of subunits were purified by SDS-PAGE and reverse-phase HPLC as described under *Materials and Methods*. A, trypsin digests of αV8–10 (Asn-339–Gly-437) were purified directly; B, purification of a 10-kDa band (α-K-10K) isolated by tricine-SDS-PAGE from Endoproteinase-Lys C digests of αV8–20 (Ser-173–Glu-338). Trypsin digests of β-, γ-, and δ-subunits were fractionated by tricine-SDS-PAGE to isolate from β-subunit 5 kDa (β-T-5K) and 7-kDa (β-T-7K) bands, from γ-subunit a 5-kDa band (γ-T-5K), and from δ-subunit a 5 kDa band (δ-T-5K). C and D, reversed-phase HPLC purification of β-T-5K and β-T-7K, respectively. E and F, purification of γ-T-5K and δ-T-5K respectively.

tending through γM4 (116 pmol) that was present at 10-fold higher level than secondary sequences that began at γLys-218 (amino terminus of γM1, 10 pmol) and at γVal-273 (amino terminus of γM3, 12 pmol). The ^{3}H released in cycles 6 and 8 indicated that [^{3}H]promegestone was incorporated into γCys-451 (2 cpm/pmol)and γTrp-453 (~0.4 cpm/pmol) within γ-M4. Incorporation into γCys-451 was also evident in the amino-terminal sequence analysis of γT-5K isolated from membranes labeled in the absence of carbamylcholine (data not shown).

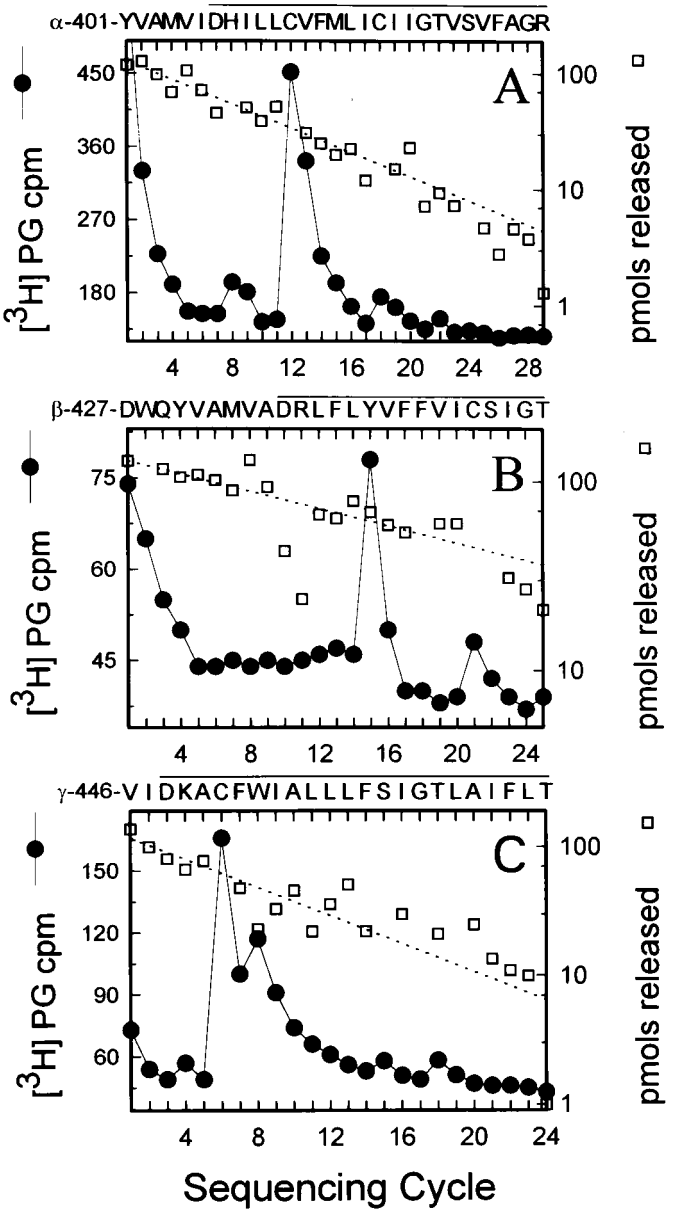

Fig. 6. Radioactivity and mass release upon amino-terminal sequence analysis of the M4 region of the α-, β-, and γ-subunits. For AChRs labeled with [^{3}H]promegestone in the presence of agonist, the M4 regions of the α- β-, and γ-subunits were isolated from tryptic digests of αV8–10 (Asn-339–Gly-437) and intact β- and γ-subunits. M4 containing proteolytic fragments α-T-4K, β-T-4K, and γ-T-5K were purified by reverse-phase HPLC (Fig. 5, A, C, and E) and the fractions containing the peaks of ^{3}H were pooled (fractions 28–32, 28–32, and 31–35, respectively) and sequenced. For each sample 60% of each cycle of Edman degradation was analyzed for released ^{3}H (●) and 30% for PTH-amino acids (□) with the dashed lines corresponding to the exponential decay fit of the amount of detected PTH-amino acids for the peptides containing M4. The amino acid sequence of the sequenced peptide containing the M4 region is shown above each panel. A, ^{3}H release from α-T-4K [I_o = 129 pmol; r = 89%; 44,000 cpm loaded/5800 remaining on filter]. B, ^{3}H release from β-T-4K [I_o = 129 pmol; r = 95%; 7700 cpm loaded/2100 remaining on filter]. C, ^{3}H release from γ-T-5K [I_o = 116 pmol; r = 88%; 7800 cpm loaded/1950 remaining on filter].

Radiochemical Sequence Analysis of M2 Segments of AChR α-, β-, and δ-subunits. Subunit proteolytic fragments beginning at the amino termini of the M2 segments of AChR α-, β-, and δ-subunits were isolated from AChRs labeled with [^{3}H]promegestone in the presence of carbamylcholine. For α-subunit, an EKC digest of αV8–20 (~280 μg) was fractionated by tricine SDS-PAGE, and an ~10- kDa fragment (α-K-10K), previously shown to contain the M2-M3 region (Pedersen et al., 1992), was isolated from the gel (see *Materials and Methods*). When the material eluted from the α-K-10K fragment was further purified by reversed-phase HPLC (Fig. 5B), the majority of ^{3}H counts eluted in a peak centered at 84% solvent B. HPLC fractions 32–35 were pooled and sequenced (Fig. 7A). The primary sequence, which began at αMet-243, the amino terminus of the M2 region (85 pmol), was present at 10-fold higher level than a secondary sequence beginning at the amino terminus of αM3 (αTyr-277, 7 pmol). No significant ^{3}H release above background was observed in any of the 21 sequencing cycles.

To identify potential sites of [^{3}H]promegestone photoincorporation in the M2 regions of β- and δ-subunits, trypsin digests of the subunits (~250 μg) were first fractionated by tricine SDS-PAGE. For the β-subunit, a 7-kDa fragment (β-T-7K), known to contain both the M2 and M3 region, was identified as a band of weak fluorescence between two strongly fluorescent bands of 10 and 5.5 kDa when the tricine SDS-PAGE gel was illuminated at 365 nm (data not shown). The material eluted from the β-T-7K band was further purified by reverse-phase HPLC (Fig. 5D), with the majority of ^{3}H counts eluting in a peak centered at 80% solvent B. Sequence analysis of the pool of HPLC fractions 30 to 34 (Fig. 7B) revealed the presence of a peptide beginning at β-Met-249, the amino terminus of the βM2 (86 pmol), along with secondary sequences beginning at the amino termini of βM1 (βLys-216, 15 pmol) and βM4 (βAsp-427, 10 pmol). No ^{3}H release above background was seen in any of the 21 sequencing cycles. Similarly, no [^{3}H]promegestone incorporation was evident in the ^{3}H release profile obtained upon sequencing the β-T-7K fragment labeled in the absence of agonist (data not shown).

When the trypsin digest of [^{3}H]promegestone-labeled δ-subunit was resolved by tricine SDS-PAGE, a 5-kDa fragment (δ-T-5K), known to contain the M2–M3 region, was identified by the use of prestained molecular weight standards and by the fluorescence associated with 1-azidopyrene incorporation into M3. When the material eluted from the δ-T-5K band was further purified by reverse-phase HPLC (Fig. 5F), the majority of ^{3}H counts eluted in a peak centered at 82% solvent B. When HPLC fractions 30 to 33 were pooled and sequenced (Fig. 7C), a primary sequence was identified beginning at δMet-257, the amino terminus of the δM2 (90 pmol), along with a secondary sequence beginning at the amino terminus of δM4 (δAsn-447, 7 pmol). No clear ^{3}H release above background was detected.

Discussion

We have shown that the synthetic progestin, promegestone, is a NCA of the *Torpedo* AChR. Promegestone reversibly inhibits ACh-elicited currents for *Torpedo* AChRs expressed in *Xenopus* oocytes with the same potency as progesterone. Because promegestone concentrations up to 100 μM increase the [^{3}H]ACh equilibrium binding affinity to AChR-rich membranes, promegestone is a desensitizing NCA. Interestingly, although it is only a weak inhibitor (IC_{50} ~ 100 μM) of [^{3}H]HTX binding to AChRs in the desensitized state, it is a potent inhibitor (IC_{50} = 9 μM) of [^{3}H]PCP binding. Because binding of HTX and PCP appear formally competitive (Heidmann et al., 1983; White et al., 1991), this result appears at first surprising. However, studies with TID, an uncharged, photoactivatable NCA, provide clear evidence that the binding sites for PCP and HTX can be differentiated (White et al., 1991; White and Cohen, 1992): TID is a potent, competitive inhibitor of [^{3}H]PCP binding to AChRs in the desensitized state, whereas it is an allosteric inhibitor of [^{3}H]HTX binding. Although HTX and PCP are presumed to bind within the lumen of the ion channel, their site(s) of high-affinity binding have not been mapped directly. The high-affinity binding site for [^{3}H]tetracaine in the AChR in the resting state has been shown by direct photoaffinity labeling to overlap with the [^{125}I]TID site in the M2 ion channel domain (White and Cohen, 1992; Gallagher and Cohen, 1994; Gallagher, 1996). Although promegestone at high concentrations (IC_{50} ~75 μM) inhibits [^{3}H]tetracaine binding, that inhibition probably occurs because promegestone stabilizes the AChR desensitized state that binds [^{3}H]tetracaine only weakly. Although promegestone clearly can be a potent inhibitor of NCA binding, the results of the radioligand assays provide no clear indication of the nature of the promegestone binding site(s) in the AChR.

When [^{3}H]promegestone was photoincorporated into AChR-rich membranes, its incorporation was readily detected in residues in the M4 segments of the α-, β-, and γ-subunits that previous work has shown are exposed to lipid (Fig. 8; Blanton and Cohen, 1994; Blanton et al., 1998). In contrast, no incorporation was detected in the sequence analysis of the α-, β-, or δ-M2 segments isolated from AChRs labeled in either the absence or presence of agonist. The simplest interpretation of the photolabeling data is that, consistent with its lipophilicity, the steroid promegestone binds to and interacts with the AChR at the lipid-protein interface. The inability of increasing doses of progesterone to affect the photoincorporation of [^{3}H]promegestone, at least at the subunit level, is also consistent with "nonspecific" binding at the lipid-protein interface. Although promegestone interaction at the AChR-lipid protein interface does not meet the classical criteria for a specific drug-receptor binding site, this does not preclude this promegestone-AChR interaction from affecting AChR function. Additional studies are re-

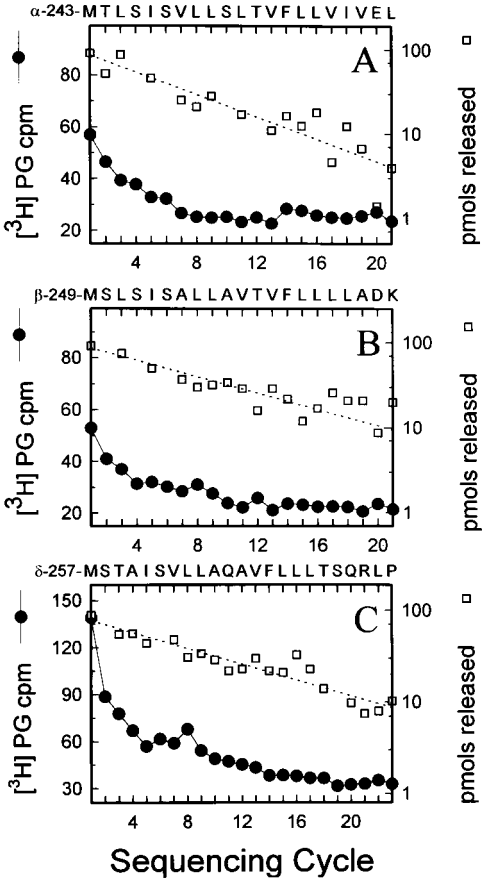

Fig. 7. Radioactivity and mass release upon amino-terminal sequence analysis of the M2 regions of α-, β-, and δ-subunits. For AChRs labeled with [^{3}H]promegestone in the presence of agonist, proteolytic fragments beginning at the amino termini of the M2 regions of the α- β-, and δ-subunits were isolated from either an EKC digest of αV8–20 (Ser-173–Glu-338) or tryptic digests of intact β- and δ-subunits. The α-K-10K, β-T-7K, and δT-5K fragments containing M2 segments isolated by tricine SDS-PAGE were further purified by reverse-phase HPLC (Figs. 5B, D, and F, respectively) and the fractions containing the peaks of ^{3}H were pooled (fractions 32–35, 30–34, and 30–33, respectively) and sequenced. For each sample 60% of each cycle of Edman degradation was analyzed for released ^{3}H(●) and 30% for PTH-amino acids (□) with the dashed lines corresponding to the exponential decay fit of the amount of detected PTH-amino acids for the each of the M2 containing peptides. The amino acid sequence of the sequenced peptides containing the M2 region is shown above each panel. A, ^{3}H release from α-K-10K [I_o = 85 pmol; r = 85.8%; 6200 cpm loaded/2000 cpm remaining on filter]. B, ^{3}H release from β-T-7K [I_o = 86 pmol; r = 90%; 3,600 cpm loaded/1000 cpm remaining on filter]. C, ^{3}H release from δ-T-5K [I_o = 90 pmol; r = 91%; 7,700 cpm loaded/1,200 cpm remaining on filter].

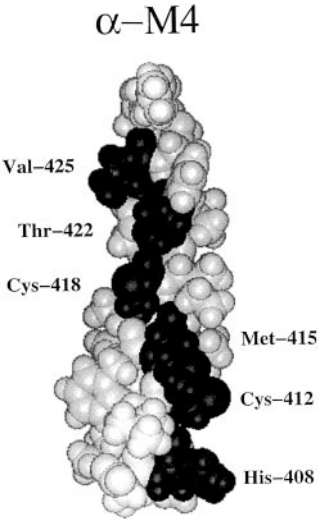

Fig. 8. Corey-Pauling-Koltun models of the α-M4 helix. The amino acids labeled by [^{3}H]promegestone (His-408, Cys-412, and Cys-418) are also labeled by the hydrophobic probe [^{3}H]diazofluorene (as is Met-415 (Blanton et al., 1998)) and by [^{125}I]TID [which also reacts with Thr-422 and Val-425 (Blanton and Cohen, 1994)].

quired to determine whether promegestone interactions at the AChR-lipid interface result in the observed inhibition of NCA binding or of ACh-induced ion currents. Also, additional studies are required to determine whether promegestone is interacting at sites on the AChR surface normally occupied by cholesterol, which is present at 15% (w/w) in the AChR-rich membranes and at an effective concentration of 1 mM. There is strong evidence that cholesterol interacts directly with AChRs and that neutral lipids are required to maintain the AChR in a state responsive to agonist (Rankin et al., 1997 and references therein). Inhibition by promegestone (or progesterone) might occur because it displaces cholesterol from a functionally important site.

Although our studies have found no evidence that [^{3}H]promegestone binds within the M2 ion channel domain, it remains possible that it binds within the channel but is incapable of photoincorporating into the predominantly aliphatic residues contained within each of the M2 segments. Promegestone photoincorporation proceeds through a "triplet state" biradical, which should readily incorporate into C–H bonds (Benisek, 1977). However, although very limited, the residues that have been shown to react with [^{3}H]promegestone [Met-759 and Met-909 (human progestin receptor); Met-622 and Cys-754 (rat glucocorticoid receptor) (Stromstedt et al., 1990); His-408, Cys-412, and Cys-418 (αM4); Tyr-441, Cys-447 (βM4); and Cys-451, Trp-453 (γM4) AChR, this report] do not include any aliphatic residues. In addition, it is also possible that there is an extracellular binding site for promegestone, but that the efficiency of [^{3}H]promegestone photoincorporation into this region was too low for us to detect. Finally, it also remains to be determined whether [^{3}H]promegestone is photoincorporated in the M1 or M3 hydrophobic segments (or in the AChR extracellular domain) because the subunit fragmentation strategies used in this study were chosen specifically to identify possible sites of incorporation in M2 and M4 segments.

By interacting with residues situated at the lipid-protein interface of the AChR, promegestone could allosterically alter the structure of the ion channel, effecting both ion conductance and binding of NCAs. Several recent reports provide support for this conclusion. Mutations at lipid-exposed residues in the M4 segment dramatically affect open channel lifetimes (Bouzat et al., 1994, 1998; Lee et al., 1994; Lasalde et al., 1996), and a mutation within the M2 ion channel domain that increases channel lifetime also increases hydrocortisone potency (Bouzat and Barrantes, 1996).

Finally, progesterone inhibits AChR activity but potentiates $GABA_A$ receptor currents in the same concentration range (EC_{50} = 26 μM, Wu et al., 1990). Given the emerging evidence of structural homology between these two receptors (reviewed in Sigel and Buhr, 1997), this raises the possibility that steroids may differentially modulate the activities of these two receptors (as well as other members of the AChR family) by interacting with residues at a common site, potentially at the lipid-protein interface. On the other hand the ACh and $GABA_A$ receptors have different steroid structure-activity relationships (Wu et al., 1990). Although these differences may simply reflect the different modulatory affects progesterone and other steroids have on these two receptors, it may also indicate separate steroid binding domains. In this respect, future studies will be aimed at identifying the site(s) of [^{3}H]promegestone incorporation in $GABA_A$ receptor subunits.

Acknowledgements

We thank Martin Gallagher for helpful comments and suggestions.

References

Benisek WF (1977) Labeling of Δ^5-3-ketosteroid isomerase by photoexcited steroid ketones. *Methods Enzymol* **46:**469–479.
Blanton MP and Cohen JB (1994) Identifying the lipid-protein interface of the *Torpedo* nicotinic acetylcholine receptor: Secondary structure implications. *Biochemistry* **33:**2859–2872.
Blanton MP, Dangott LJ, Raja SK, Lala AK and Cohen JB (1998) Probing the structure of the nicotinic acetylcholine receptor ion channel with the uncharged photoactivable compound [^{3}H]diazofluorene. *J Biol Chem* **273:**8659–8668.
Bouzat C, Roccamo, AM, Garbus, I. and Barrantes FJ (1998) Mutations at lipid-exposed residues of the acetylcholine receptor affect its gating kinetics. *Mol Pharmacol* **54:**146–153.
Bouzat C and Barrantes FJ (1996) Modulation of muscle nicotinic acetylcholine receptors by the glucocorticoid hydrocortisone—Possible allosteric mechanism of channel blockade. *J Biol Chem* **271:**25835–25841.
Bouzat C, Bren N and Sine SM (1994) Structural basis of the different gating kinetics of fetal and adult acetylcholine receptors. *Neuron* **13:**1395–1402.
Boyd ND and Cohen JB (1984) Desensitization of membrane-bound *Torpedo* acetylcholine receptor by amine noncompetitive antagonists and aliphatic alcohols: Studies of [^{3}H]-acetylcholine binding and ^{22}Na+ ion fluxes. *Biochemistry* **23:**4023–4033.
Bullock AE, Clark AL, Grady SR, Robinson SF, Slobe BS, Marks MJ and Collins AC (1997) Neurosteroids modulate nicotinic receptor function in mouse striatal and thalamic synaptosomes. *J Neurochem* **68:**2412–2423.
Cleveland DW, Fischer SG, Kirschner MW and Laemmli UK (1977) Peptide mapping by limited proteolysis in sodium dodecyl sulfate and analysis by gel electrophoresis. *J Biol Chem* **252:**1102–1106.
Cohen JB, Medynski DC and Strnad NP (1985) Interactions of local anesthetics with nicotinic acetylcholine receptors, in *Effects of Anesthesia* (Covino B, Fozzard H, Redher K and Strichartz G eds.) pp 53–64, American Physiological Society, Bethesda, MD.
Franks NP and Lieb WR (1994) Molecular and cellular mechanisms of general anaesthesia. *Nature(London)* **367:**607–614.
Gallagher MJ (1996) Binding domains for noncompetitive antagonists in the nicotinic acetylcholine receptor ion channel. PhD Thesis, Washington University, St. Louis, MO.
Gallagher MJ and Cohen JB (1994) Identification of amino acids involved in the binding of [^{3}H]tetracaine to the *Torpedo* nicotinic acetylcholine receptor (Abstract). *Biophys J* **66:**212.
Gee KW, McCauley LD and Lan NC (1995) A putative receptor for neurosteroids on the $GABA_A$ receptor complex: The pharmacological properties and therapeutic potential of epalons. *Crit Rev Neurobiol* **9:**207–227.
Gillo B and Lass Y (1984) The mechanism of steroid anaesthetic (alphaxalone) block of acetylcholine-induced ionic currents. *Br J Pharmacol* **82:**783–789.
Harrison NL, Majewska MD, Harrington JW and Barker JL (1987) Structure-activity relationships for steroid interaction with the γ-aminobutyric acid A receptor complex. *J Pharmacol Exp Ther* **241:**346–353.
Heidmann T, Oswald RE and Changeux J-P (1983) Multiple sites of action for noncompetitive blockers on acetylcholine receptor rich membrane fragments from *Torpedo marmorata*. *Biochemistry* **22:**3112–3127.
Hucho F, Tsetlin VI and Machold J (1996) The emerging three-dimensional structure of a receptor—The nicotinic acetylcholine receptor. *Eur J Biochem* **239:**539–557.
Ke L and Lukas RJ (1996) Effects of steroid exposure on ligand binding and functional activities of diverse nicotinic acetylcholine receptor subtypes. *J Neurochem* **67:**1100–1112.
Laemmli UK (1970) Cleavage of structural proteins during the assembly of the head of bacteriophage T4. *Nature* **227:**680–685.
Lambert JJ, Belelli D, Hill-Venning C, Callachan H and Peters JA (1996) Neurosteroid modulation of native and recombinant $GABA_A$ receptors. *Cell Mol Neurobiol* **16:**155–179.
Lambert JJ, Belelli D, Hill-Venning C and Peters JA (1995) Neurosteroids and GABA(A) receptor function. *Trends Pharmacol Sci* **16:**295–303.
Lasalde JA, Tamamizu S, Butler DH, Vibat C, Hung B and McNamee MG (1996) Tryptophan substitutions at the lipid-exposed transmembrane segment M4 of *Torpedo californica* acetylcholine receptor govern channel gating. *Biochemistry* **33:**14139–14148.
Lee Y, Li L, Lasalde J, Rojas L, McNamee M, Ortiz-Miranda SI and Pappone P (1994) Mutations in the M4 domain of *Torpedo californica* acetylcholine receptor dramatically alter ion channel function. *Biophys J* **66:**646–653.
MacDonald RL and Olsen RW (1994) $GABA_A$ Receptor Channels. *Annu Rev Neurosci* **17:**569–602.
Nurowska E and Ruzzier F (1996) Corticosterone modifies the murine muscle acetylcholine receptor channel kinetics. *NeuroReport* **8:**77–80.
Pedersen SE, Dreyer EB and Cohen JB (1986) Location of ligand binding sites on the nicotinic acetylcholine receptor α-subunit. *J Biol Chem* **261:**13735–13743.
Pedersen SE, Sharp SD, Liu W-S and Cohen JB (1992) Structure of the noncompetitive antagonist binding site in the *Torpedo* nicotinic acetylcholine receptor: [^{3}H]Meproadifen mustard reacts selectively with α-subunit Glu-262. *J Biol Chem* **267:**10489–10499.
Rankin SE, Addona GH, Kloczewiak, MA, Bugge B and Miller KW (1997) The

cholesterol dependence of activation and fast desensitization of the nicotinic acetylcholine receptor. *Biophys. J* **73:**2446–2455.
Sadler SE and Maller JL (1982) Identification of a steroid receptor on the surface of *Xenopus* oocytes by photoaffinity labeling. *J Biol Chem* **257:**355–361.
Schagger H and von Jagow G (1987) Tricine-sodium dodecyl sulfate-polyacrylamide gel electrophoresis for the separation of proteins in the range from 1 to 100 kDa. *Anal Biochem* **166:**368–379.
Sigel E and Buhr A (1997) The benzodiazepine binding site of $GABA_A$ receptors. *Trends Pharmacol Sci* **18:**425–429.
Stromstedt P, Berkenstam A, Jornvall H, Gustafsson J and Carlstedt-Duke J (1990) Radiosequence analysis of the human progestin receptor charged with [^{3}H]promegestone. *J Biol Chem* **265:**12973–12977.
Twyman RE and MacDonald RL (1992) Neurosteroid regulation of $GABA_A$ receptor single channel kinetic properties of mouse spinal cord neurones in culture. *J Physiol (London)* **456:**215–245.
Valera S, Ballivet M and Bertrand D (1992) Progesterone modulates a neuronal nicotinic acetylcholine receptor. *Proc Natl Acad Sci USA* **89:**9949–9953.
White BH and Cohen JB (1988) Photolabeling of membrane-bound *Torpedo* nicotinic acetylcholine receptor with the hydrophobic probe 3-trifluoromethyl-3-(m-[^{125}I]iodophenyl)diazirine. *Biochemistry* **27:**8741–8751.
White BH and Cohen JB (1992) Agonist-induced changes in the structure of the acetylcholine receptor M2 regions revealed by photoincorporation of an uncharged nicotinic non-competitive antagonist. *J Biol Chem* **267:**15770–15783.
White BH, Howard S, Cohen SG and Cohen JB (1991) The hydrophobic photoreagent 3-(trifluoromethyl)-3-(m-[^{125}I]iodophenyl)diazirine is a novel noncompetitive antagonist of the nicotinic acetylcholine receptor. *J Biol Chem* **266:**21595–21607.
Wu F, Gibbs TT and Farb DH (1990) Inverse modulation of γ-aminobutyric acid- and glycine-induced currents by progesterone. *Mol Pharmacol* **37:**597–602.
Zhu WJ and Vicini S (1997) Neurosteroid prolongs $GABA_A$ channel deactivation by altering kinetics of desensitized states. *J Neurosci* **17:**4022–4031.

Send reprint requests to: Dr. Jonathan B. Cohen. Department of Neurobiology, Harvard Medical School, 220 Longwood Ave., Boston MA 02115. E-mail: jonathan_cohen@hms.harvard.edu